Elastic wave properties of carbonate marine sediments in the Strait of Hormuz

A. I. Best[1], S. G. Marks[2]

[1] Challenger Division, Southampton Oceanography Centre, European Way, Southampton, SO14 3ZH, UK.
aib@soc.soton.ac.uk
[2] DERA Unit, Southampton Oceanography Centre, European Way, Southampton, SO14 3ZH, UK.
sgma@soc.soton.ac.uk

Abstract

Shallow water carbonate sediments have very different mineralogical and textural properties to siliciclastic sediments that may lead to different elastic wave properties. In situ seafloor shear wave and laboratory compressional wave measurements on the muddy, carbonate sands and gravels encountered in the Strait of Hormuz showed marked decreases in velocity and attenuation with increasing mud content. Modelling elastic properties based on mud content suggests that grainsize distribution is the dominant factor over mineralogy and grain shape.

1. Introduction

An experimental study was carried out to quantify the elastic wave propagation properties of seafloor sediments encountered in the Strait of Hormuz. The work was done in conjunction with sidescan sonar and acoustic profiler mapping of seabed and shallow sub-bottom features [1]. The Hormuz sediments are of interest because of their warm (20 - 22°C), high salinity (37 - 44 psu), shallow (40 - 200 m) water location and their high carbonate content (> 70%). In fact, the sediments comprise poorly sorted, shelly sands and gravels with 0 - 73% mud (clay and silt grade material).

Experimental and theoretical work by Marion *et al.* [2] on silica sand-clay mixtures has demonstrated an interdependence of P-wave velocity on porosity, which is related to grainsize distribution. This model was developed to explain the observed changes in P-wave velocity with shale content in sandstone-shale rocks with application to hydrocarbon exploration seismology. Given the prevalence of mud in the Hormuz sediments, the Marion model seemed appropriate for testing whether the same relationships explain variations in P-wave velocity in these carbonate-rich sediments, or whether other factors are more important, such as mineralogy and grain shape. The sand and gravel-grade grains in the Hormuz sediments show a wide range of shapes, from intact gastropod tests, ooids and peloids with intra-granular porosity, to broken shell fragments with no intra-granular porosity. It is not obvious that such a material will behave acoustically in the same manner as a muddy silica sand, for example, with its mainly solid quartz grains. It is known that intra-test porosity can complicate P-wave velocity/porosity relationships in deep ocean pelagic carbonates [3] and this is generally not the case for siliciclastic sediments [4].

2. Seismo-acoustic measurements

2.1 *In situ* surface shear wave measurements

In situ shear wave measurements were obtained in April 1997 at eight sites straddling the main shipping channel (Figure 1) using the newly developed SAPPA (Sediment Acoustic and Physical Properties Apparatus [5]). In order to generate horizontally polarised surface shear waves, a shear plate (10 cm x 15 cm) was held in firm contact with the seafloor and struck in alternate directions in the horizontal plane by two miniature hammers. A three-component geophone receiver was similarly coupled to the seafloor at a distance of 1.18 m from the source. Horizontally polarised surface shear wave arrivals were clearly identifiable and their first break times, peak amplitudes and dominant frequencies were recorded. Two separate SAPPA deployments were made at each seafloor site to improve confidence in the results. Attenuation was computed using a reference signal measured on wet, quartz sand on West Wittering beach in the UK using the same source and receiver, detached from the SAPPA frame. By measuring the signal amplitude decay with offset up to 10 m, it was possible to find the intrinsic attenuation coefficient of the beach sand, although a cylindrical spreading law had to be assumed.

The results [6] show that the majority of the SAPPA sites have low shear wave velocities (11 - 20 m/s) and high attenuations (1000/Qs: 66 to 164); seafloor samples indicate significant mud contents (15 - 73%). The other sites show higher velocities and occur in areas with lower mud contents. Site S06 has the highest velocity and

TG Leighton, GJ Heald, HD Griffiths, G Griffiths, (eds.), 'Acoustical Oceanography', Proc. Institute of Acoustics Vol. 23 Part 2, 2001.

attenuation of all the SAPPA sites and seafloor samples indicate very coarse sand and gravel there. The dominant signal frequency varies between 35 Hz for the muddy sediments and 216 Hz for S06, giving a constant wavelength of 0.57 m.

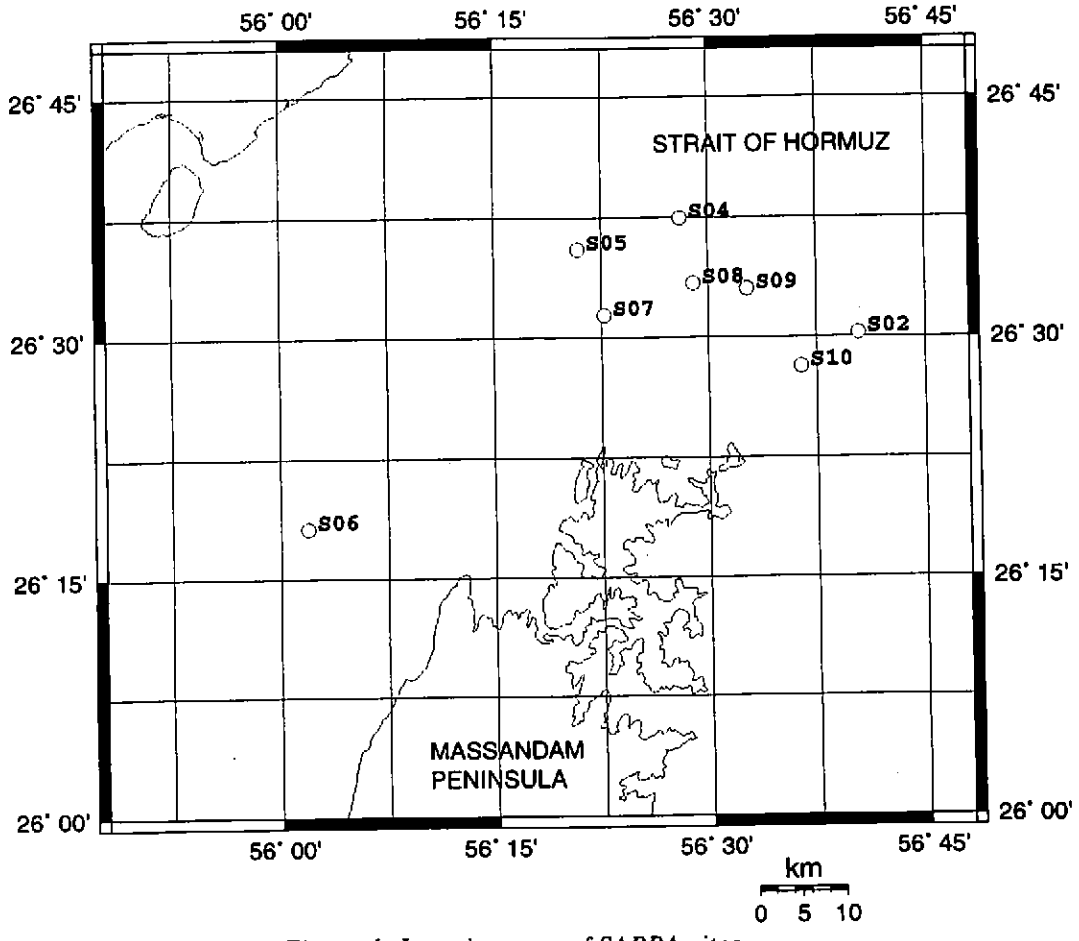

Figure 1. Location map of SAPPA sites

2.2 Laboratory P-wave measurements

No *in situ* P-wave measurements were made because of equipment problems at sea, so laboratory P-wave measurements were performed on seafloor samples instead. A water tank transmission method was used comprising two identical broadband, piezoelectric transducers (500 kHz, 2.54 cm diameter) as transmitter and receiver with the sediment sample contained in a perspex-walled box (10 cm x 10 cm x 2 cm) and suspended between them in the water tank. The frequency dependent phase velocity and attenuation of the sediment were calculated relative to the signal recorded through the water-filled box using either a broadband transient pulse or a single frequency sinusoid as the transmitted signal. The results reported below were obtained by identifying phase points (e.g. peaks or troughs) on single frequency sinusoidal pulses.

Initial results [6] show that P-wave velocity decreases with increasing mud content and indicate that P-wave attenuation (Qp^{-1}) follows a similar trend.

3. Comparison with siliciclastic sediments

The Hormuz laboratory P-wave results were corrected to an *in situ* temperature of 22°C using the seawater velocity-temperature relationship and compared to published P-wave data. The DERA GEOSEIS database is a quality controlled compilation of seismo-acoustic, geotechnical and geochemical data obtained from the open literature, and a dedicated measurement programme [7]. GEOSEIS contains over 100,000 records from 73 sources and was used to provide comparative data for siliciclastic and carbonate sediments. The GEOSEIS data in Figure 2 show similar velocity-porosity relationships for both siliciclastic and carbonate marine sediments with relatively few outliers. It appears that the shallow water, Hormuz, carbonate sediments behave acoustically like siliciclastic marine sediments, showing a similar range of P-wave velocities for a given porosity. The Lower Florida Keys data [8] also show a similar trend.

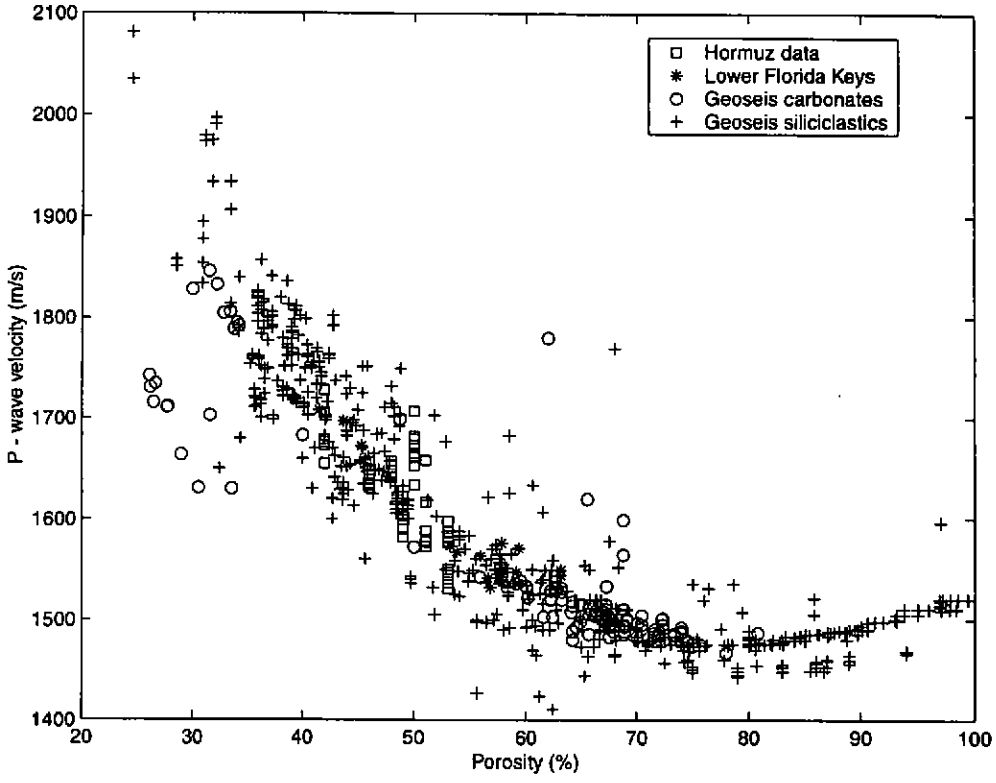

Figure 2. Hormuz sediment P-wave velocity versus porosity corrected to an in situ temperature of 22 °C. Also shown are data for carbonate and siliciclastic sediments from the Geoseis database, and in situ Florida Keys data from Richardson et al. [8].

4. Modelling P- and S-wave velocity on mud content

Marion *et al.* [2] developed a simple model of P-wave velocity in sand/shale mixtures that showed good agreement with experimental results in unconsolidated sand/clay mixtures, shaly sandstones and sandy shales. The model was adapted here for mud content, that is the total volume percentage of clay and silt grade material, and sand content, taken here to include both sand and gravel grade material. The model is based on the physical relationship between packing (hence porosity) and the grain diameter ratio of binary mixtures of fine and coarse spheres. When the ratio of coarse/fine spheres is greater than about 100, the packing approaches its ideal state and the fine spheres do not interfere with the packing of the coarse spheres. The reverse is true when this ratio is very small. The two end members of this model are represented in Figure 3, namely, muddy sand and sandy mud.

This model of spherical grains approximates siliciclastic sediments quite well (e.g. well rounded quartz grains), but does not approach the reality of the Hormuz carbonate sediments with their mixture of sub-rounded peloids and ooids, and elongate shell fragments (although the Hormuz sediments do show bimodal grainsize distributions).

The model leads to two expressions for porosity ϕ based on the mud content m, the porosity of the pure sand (and gravel) ϕ_s, and the porosity of the pure mud ϕ_m. For $m \leq \phi_s$ (i.e. for muddy sands):

$$\phi = \phi_s - m(1-\phi_m); \tag{1}$$

and for $m > \phi_s$ (i.e. for sandy muds):

$$\phi = m\phi_m. \tag{2}$$

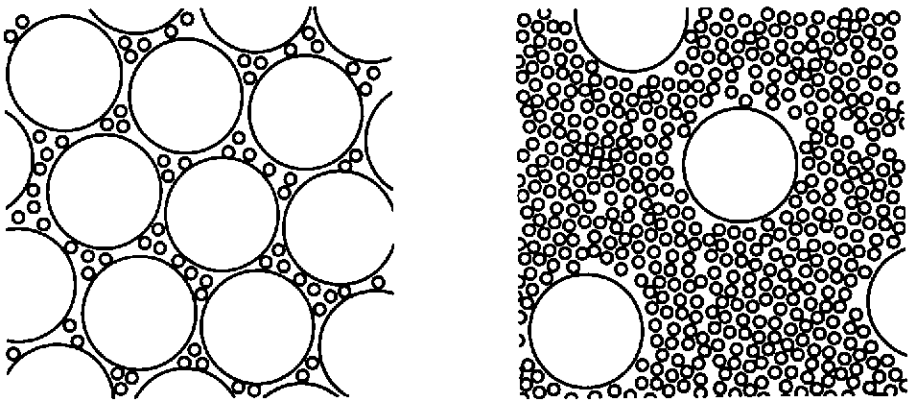

Figure 3. The two end members of the porosity model: muddy sand and sandy mud. The large circles represent "sand" grains (sand and gravel), and the small circles mud grains (clay and silt grade material).

The mud content in the model is expressed as a volume ratio, but mud content is generally measured as a mass ratio during grainsize analysis; Marion *et al.* [2] give expressions for converting the model mud contents to mass percentages. The model uses the computed porosities to calculate the sediment bulk density ρ, sediment bulk modulus K, and sediment shear modulus G with the relations of Gassmann [9] for muddy sand and the Reuss [10] elastic moduli averages for sandy mud as follows. For $m \leq \phi_s$ (i.e. for muddy sands):

$$\frac{K}{K_s - K} = \frac{K_b}{K_s - K_b} + \frac{K_f}{\phi_s (K_s - K_f)}, \tag{3}$$

$$G = G_b, \tag{4}$$

$$\rho = (1-\phi_s)\rho_s + m(1-\phi_m)\rho_m + (\phi_s - m(1-\phi_m))\rho_w, \tag{5}$$

where, K_s, K_f and K_b are the bulk moduli of the grain forming mineral, the pore filling material and the framework of interlocking grains (hereafter referred to as the "frame"), respectively; Gb is the shear modulus of the frame; and ρ_s, ρ_m and ρ_w are the densities of the grain forming mineral, mud-forming minerals (excluding pore water, but including clay bound water), and saturating fluid, respectively. For $m > \phi_s$ (i.e. for sandy muds):

$$\frac{1}{K} = \frac{m}{K_m} + \frac{1-m}{K_s}, \tag{6}$$

$$\frac{1}{G} = \frac{m}{G_m} + \frac{1-m}{G_s}, \tag{7}$$

$$\rho = (1-m)\rho_s + m(1-\phi_m)\rho_m + m\phi_m\rho_w, \tag{8}$$

where, K_m and G_m are the bulk and shear moduli of the saturated mud, respectively. Implementation of the model requires knowledge of K_b, G_b, K_f, K_m, G_m, ρ_m, ϕ_s and ϕ_m as the remaining parameters (K_s, G_s, ρ_s, ρ_w) can be obtained from standard tables.

5. Model implementation

In practice, obtaining sensible values for the input parameters is not straightforward. Unlike the sand-shale case of Marion *et al.* [2], there are no experimental data available for the pure sand and pure mud end members of the Hormuz sediments. The best that was achievable for the Hormuz sediments was to use the laboratory P-wave velocity V_p of the sandiest sample (CD104/130; 91% sand; 9% gravel; 40% porosity) and muddiest sample (CD104/61; 65% mud; 35% sand; 0% gravel; 61% porosity), together with an estimate of S-wave velocity V_s from the SAPPA data (assuming no frequency dependence) and the relationships:

$$V_p = \sqrt{\frac{K + \frac{4G}{3}}{\rho}}, \tag{9}$$

$$V_s = \sqrt{\frac{G}{\rho}}. \tag{10}$$

This leads to best estimates of K_b and G_b using (3) and (4). Similarly, the values of K_m and G_m were obtained using (9) and (10) for the muddiest sample. The value of K_f for muddy sands depends on the percentage of the sand pore space filled by mud, and hence will be a function of mud porosity. Marion *et al.* [2] used a relationship between K_f and shale porosity derived from V_p and V_s measurements at increasing effective pressures (thus compacting the shale and reducing porosity). Similar expressions were adopted for the pure Hormuz mud:

$$\frac{1}{K_f} = \frac{1-\phi_{pf}}{K_1} + \frac{\phi_{pf}}{K_2}, \tag{11}$$

$$\phi_{pf} = \frac{\phi_s - m(1-\phi_m)}{\phi_s}, \tag{12}$$

where, ϕ_{pf} is the porosity of the pore filling material; and K_1 and K_2 are the bulk moduli of pure mud at 0% and 100% porosity, respectively. The parameter K_1 was derived by linear extrapolation knowing the bulk modulus of sea water (K_2 = 2.25 GPa) and that of the muddiest sample (CD104/61) at a porosity of 60%. The value for K_m was calculated in the same manner as for K_f, as they amount to the same thing (i.e. the bulk modulus of the pure mud as a function of porosity and mud content). The value of G_m was taken as the shear modulus of the muddiest sample CD104/61 and was assumed to stay constant with porosity and mud content, in a similar manner to G_b in (4). Table 1 lists the input parameters used to model the Hormuz sediments.

The Hormuz sediment porosities are plotted against mud content (mass percent) in Figure 4 together with the initial model results (Model A) and the improved model results (Models B and C). The initial model poorly fits the data because it does not account for the fact that the introduction of mud into the sand frame will increase the sand frame porosity; not all the mud will fall into the pore space, but some will locate between sand grains. Similarly, the mud frame porosity will increase as sand content increases (decreasing mud content) because mud in the vicinity of sand grains will tend to become disturbed. The improved model takes this account by letting ϕ_s and ϕ_m vary in a linear fashion between their minimum and maximum values; the latter occur at the critical porosity when $m = \phi_{smax}$. Unfortunately, this introduces another two unknowns into the model, ϕ_{smax} and ϕ_{mmax}. These must be determined by fitting the model curve to the data, as was done for the Model B (fitted to porosity data: ϕ_{smax} = 49%, ϕ_{mmax} = 90%) and Model C (fitted to P-wave velocity data: ϕ_{smax} = 49%, ϕ_{mmax} = 86%) in Figures 4 and 5.

Parameter	Value	Comments
ϕ_s	0.45	Estimate from sandiest samples.
ϕ_m	0.60	Estimate from muddiest samples.
K_s	74.8 GPa	Calcite.
G_s	30.6 GPa	Calcite.
K_m	-	Calculated as for K_f.
G_m	400 kPa	SAPPA data estimate for muddiest samples.
K_1	30.0 GPa	Linear extrapolation of known values.
K_2	2.25 GPa	Sea water
K_b	0.0231 GPa	Estimate for sandiest samples.
G_b	720 kPa	Estimate for sandiest samples.
ρ_s	2450 kg/m^3	Measured on sample CD104/130.
ρ_m	2410 kg/m^3	Measured on sample CD104/61.
ρ_w	1024 kg/m^3	Sea water.

Table 1. Model A input parameters

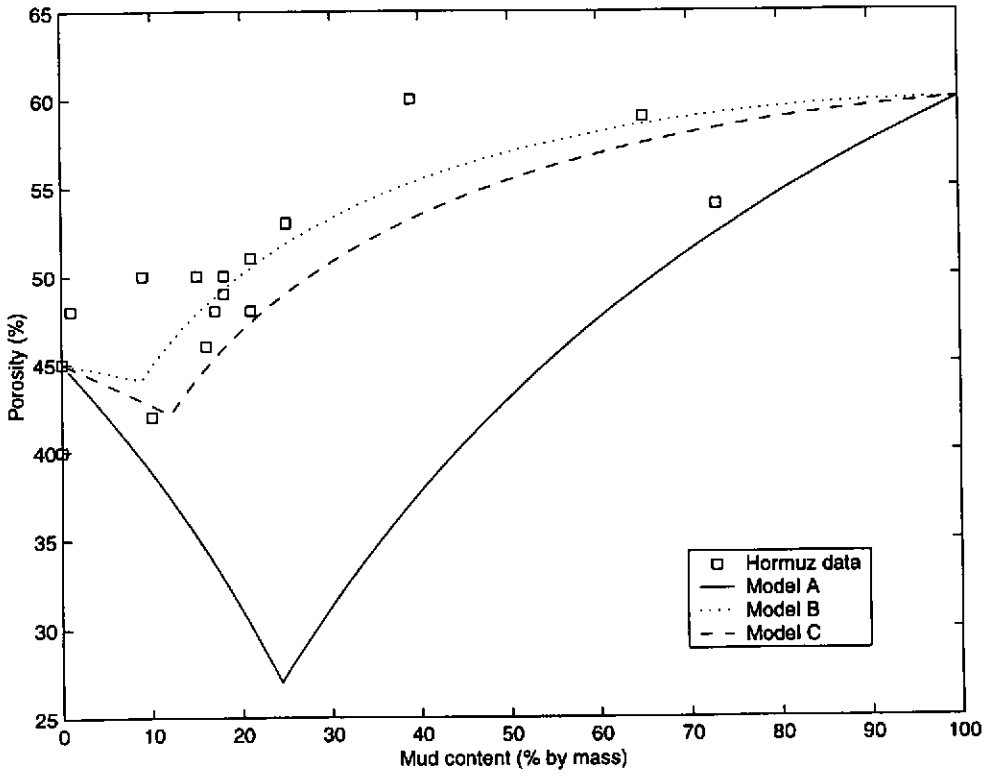

Figure 4. Porosity versus mud content for the Hormuz sediments with model results

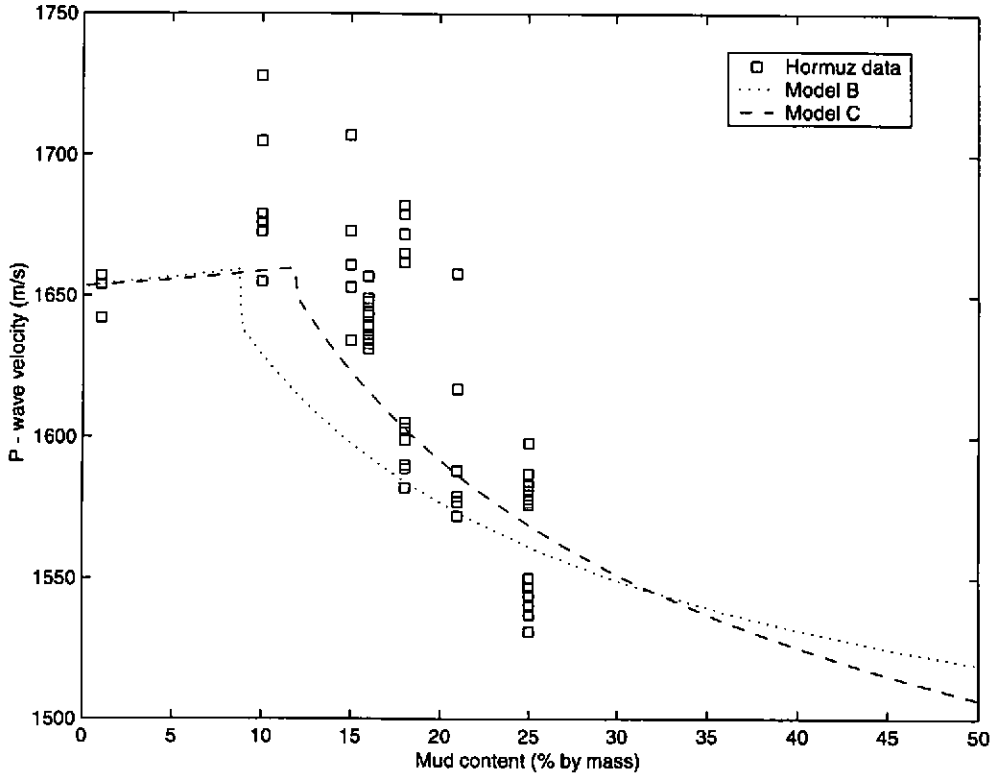

Figure 5. P-wave velocity versus mud content

6. Discussion of results

The data in Figures 4 and 5 are sparse and are complicated by the fact that not every sample has a complete set of grainsize, porosity and P-wave velocity values. However, the model can be fitted to the porosity/mud content data using input parameters based on sample measurements. The best fit Model B predicts a critical mud content of 9% and a minimum porosity of 44% although the data do not resolve this detail. This same model underestimates P-wave velocity for mud contents between about 12% – 17% in Figure 5. Conversely, the best fit model for the velocity/mud content data underestimates porosity in Figure 4. This suggests that there is some other factor affecting the relationships among P-wave velocity, porosity, and mud content, but it is probably of secondary importance. Intra-granular porosity is a strong candidate for this as many of the sand grains comprise whole or partial shells with obvious intra-test porosity when viewed in thin section. In fact, to account for the velocity of the muddy sand ($m \leq \phi_{xmax}$), it was necessary to use the measured grain density of 2450 kg/m^3 and a grain bulk modulus (K_r) of 12.14 GPa that was calculated using the Reuss average method [10]. Assuming the difference in measured grain density and that of calcite (2710 kg/m^3) is due to intra-granular porosity gives an intra-granular porosity of 15%, which can be used to compute the Reuss average grain bulk modulus. However, using this new grain bulk modulus to compute the P-wave velocity of sandy mud ($m > \phi_{xmax}$) drastically underestimates the experimental velocities; the original value for calcite was used instead for sandy mud. This suggests that the sand component of sandy mud has insignificant intra-granular porosity.

The P-wave velocity was measured at several frequencies between 200 – 600 kHz for each sample and shows a range of values for each mud content in Figure 5. Ultrasonic scattering may be partly responsible for the observed frequency dependence in these coarse grained sediments (velocities decrease by about 1.5% with increasing frequency) and these results are still being assessed.

Another aspect not discussed here, but part of the study, is the effect of mud content on S-wave velocity. Richardson *et al.* [8] noted that the shallow water carbonates of the Lower Florida Keys had significantly different

velocity-porosity trends to siliciclastic sediments. The mud content/porosity relationship above may be used as a basis for formulating expressions for S-wave velocity, although more work is needed to establish the nature of the G_b - mud content relationship.

7. Conclusions

The muddy carbonate sands found in the Strait of Hormuz exhibit a P-wave velocity-porosity relationship similar to those of many other marine sediments, both siliciclastic and carbonate, from deep and shallow water. Model results confirm that the porosity of the Hormuz sediments is primarily a function of mud content, although there is evidence of a secondary effect due to intra-granular porosity. A critical mud content of between 9% - 12% is predicted where porosity is at a minimum of between 42% - 44%, although the data are too sparse to resolve this feature. The model predicts the trends seen in the velocity data, and is able to match the velocity magnitudes after adjustment of the sand grain density and grain elastic modulus for intra-granular porosity in muddy sands. Interestingly, the model results imply that intra-granular porosity is not as important in the sandy mud component of the system. The next stage is to study the effect of mud/porosity relations on S-wave velocity (i.e. frame shear modulus).

The frequency dependence of P- and S-wave velocity was assumed to be negligible here for the purpose of obtaining estimates of the model input parameters, which may not always be the case. More well constrained datasets of P-wave and S-wave velocity and attenuation over different frequency ranges are needed to address this issue.

8. Acknowledgements

This work was funded by the United Kingdom (UK) Natural Environment Research Council, and the UK Defence and Evaluation Research Agency.

References

[1] Kenyon NH. RRS Charles Darwin Cruise 104 Leg 2, 21 March - 19 April 1997. Geological processes in the Strait of Hormuz, Arabian Gulf: a contribution to the Scheherezade Programme. Southampton Oceanography Centre, Southampton, 1997, pp. 61

[2] Marion D, Nur A, Yin H and Han D. Compressional velocity and porosity in sand-clay mixtures. *Geophysics* 1992; **57 (4)**: 554-563

[3] Urmos J and Wilkens RH. In situ velocities in pelagic carbonates: new insights from Ocean Drilling Program Leg 130, Ontong Java Plateau. *Journal of Geophysical Research* 1993; **98 (B5)**: 7903-7920

[4] Hamilton EL. Elastic properties of marine sediments. *Journal of Geophysical Research* 1971; **76 (2)**: 579-604

[5] Best AI, Roberts JA, and Somers ML. A new instrument for making *in situ* acoustic and geotechnical measurements in seafloor sediments. *Journal of the Society for Underwater Technology* 1999; **23 (3)**: 123-131

[6] Best AI and Marks SG. Elastic wave properties of carbonate marine sediments in the Strait of Hormuz, in *Proceedings of the Fifth European Conference on Underwater Acoustics,* Lyon, France, European Commission, 2000, Volume 2, pp. 819-824

[7] McCann C, McDermott I, Grimbleby L, Marks S, McCann D and Hughes B. The GEOSEIS database: a study of the acoustic properties of sediments and sedimentary rocks, in *Oceanology International Conference Abstracts*, Brighton, UK, 1994

[8] Richardson MD, Lavoie DL and Briggs KB. Geoacoustic and physical properties of carbonate sediments of the Lower Florida Keys. *Geo-Marine Letters* 1997; **17**: 316-324

[9] Gassmann F. Elastic waves through a packing of spheres. *Geophysics* 1951; **16**: 673-685

[10] Reuss A. Berechnung der fliessgrense von mischkristallen auf grund der plastizitatsbedingung für einkristalle. *Zeitschrift für Angewandte Mathematik und Mechanik* 1929; **9**: 49-58